

SHOCK WAVE BOUNDARY LAYER INTERACTION IN PROFILE CASCADES REPRESENTING ROTOR BLADINGS OF THE LAST STAGE OF LARGE OUTPUT STEAM TURBINES

Martin LUXA¹, David ŠIMURDA¹, Jaromír PŘÍHODA¹ and Jana VÁCHOVÁ²

¹ Institute of Thermomechanics, AS CR, v.v.i.
Dolejskova 5, Prague 8, The Czech Republic
e-mail: luxa@it.cas.cz, simurda@it.cas.cz, prihoda@it.cas.cz

² Doosan Skoda Power Co. Ltd.
Tylova 57/1, Pilsen, The Czech Republic
e-mail: jana.vachova@doosan.com

Keywords: shock wave-boundary layer interaction, long turbine blade, large output steam turbine, last stage

Abstract: *This paper is mainly focused on selected interaction phenomena occurring in the root, middle and tip section of the last stage rotor blading consisting of titanium blades Doosan Skoda 1375mm (54") and steel blades Doosan Skoda 1220mm (48"). Measurements and CFD simulations of the flow in selected sections along the blading radius show different types of interaction. Typically for the parts of the blade closer to the hub, only interaction of internal branch of exit shock wave with the suction side boundary layer takes place. At the blade tip where the flow is supersonic at both inlet and outlet, interaction of internal branch of inlet shock wave with the pressure side boundary layer occurs. The "reflected", additional shock wave arising from this interaction affect the flow field close to the suction side of the adjacent profile. The structure of interaction often depends on the flow conditions (nominal conditions and off-design conditions of flow, incl. different inlet flow angles).*

1 INTRODUCTION

Major part of modern, ultra long turbine rotor blades, which are designed for the last stages of low pressure cylinder in steam turbines of large output, operate in transonic and supersonic regimes of flow. The shock wave/ boundary layer interaction takes place along the major part of the blade (or even along the whole blade). The situation of Mach number distribution in the last stage of the low pressure cylinder of large output steam turbine is shown the Fig. 1. The inlet relative velocity for the titanium blade 54" reaches sonic condition approximately at the 85% of the blade height and relative exit velocities downstream the titanium blade are supersonic along the whole blade. The whole interblade channel is under nominal conditions aerodynamically choked. A small closed local region of supersonic velocity in the interblade channel, which occurs at the root section, extends upstream progressively along the blade height and covers larger part of interblade channel (see Fig. 2).

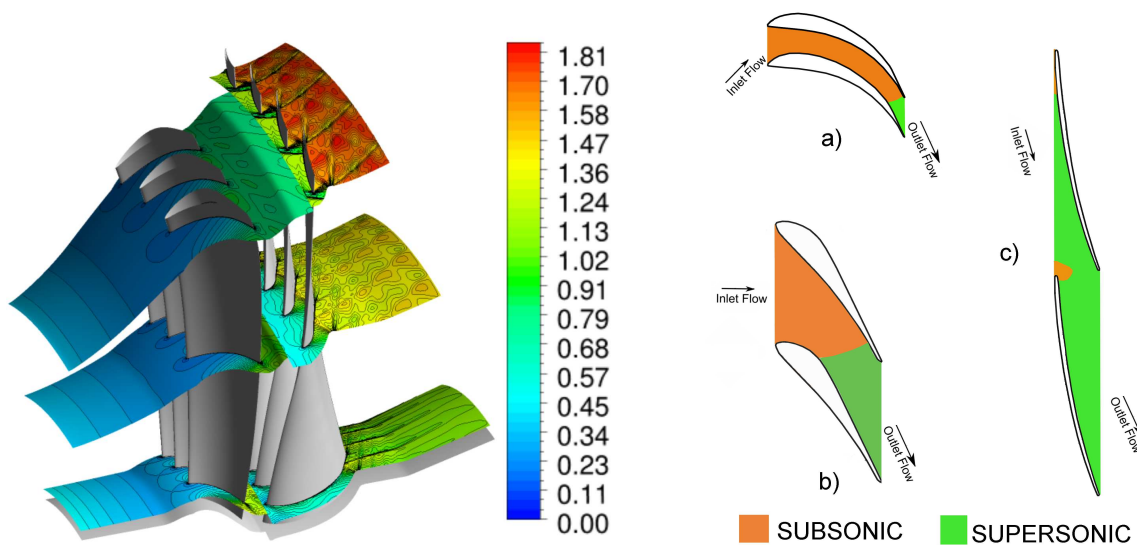


Figure 1: Mach number distribution along the blades in the last stage of low pressure cylinder with rotor titanium blade 1375mm (54").

Figure 2: Proportion of supersonic and subsonic parts of flow field in long rotor turbine blade 54" (hub - a, midsection - b, tip - c).

In the tip region, the flow field is completely supersonic (except a small subsonic region near the leading edge downstream the inlet shock wave). Typical shock wave/boundary layer interaction, which occurs approximately along the whole blade height (considering the blade root), is interaction of internal branch of exit shock wave with boundary layer on the suction side of neighbouring blade (first interaction region) - see sign 1 in Fig. 3. Situation is much more complex in the tip region. In addition to this interaction, the interaction of internal branch of inlet shock wave upstream the profile leading edge with boundary layer on pressure side of previous profile often takes place. It is typical for this second interaction region, that new "reflected" shock wave arises which interacts with boundary layer on the opposite side of interblade channel, i.e. with boundary layer on the suction side of the blade (third interaction region). In some cases of the tip profile cascades (for higher inlet Mach numbers), the oblique internal branch of inlet shock is so significantly bent, that it misses suction side of the previous profile and propagates through the wake downstream the blade row and thus only the interaction of internal branch of exit shock wave with boundary layer on the suction side of neighbouring blade occurs.

Interaction with turbulent boundary layer in the first interaction region is often observed in experiments. However, the character of the interaction can be changed under different off-

design flow conditions. This is mainly due to changes of inlet flow angle, which generate not only different boundary layer formation and development on the suction side of the blade, but - logically - also different position of the boundary layer transition. Characteristic for the second interaction region in investigated tip cascades is the interaction with laminar or transitional boundary layer. It is therefore very useful to apply proper transitional models of turbulence in the CFD simulations. These models predict the situation in the flow field, which is observed at optical and pneumatic experiments in aerodynamic wind tunnel in Aerodynamic laboratory of Institute of Thermomechanics in Nový Knín significantly better. Finally, in the third region, interaction with turbulent boundary layer appears in interferograms and schlieren pictures.

Parallel application of both different methods of measurements and commercial and in-house developed codes of CFD effectively leads not only to significantly more complex information regarding the transonic complex flow field in closed curved channel but also to rapid development of numerical and experimental techniques.

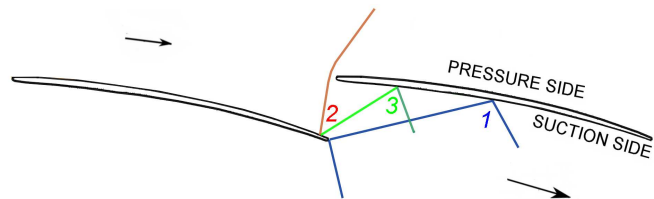


Figure 3: Three regions of shock wave - boundary layer interaction in the tip section of long turbine blade with supersonic inlet velocity

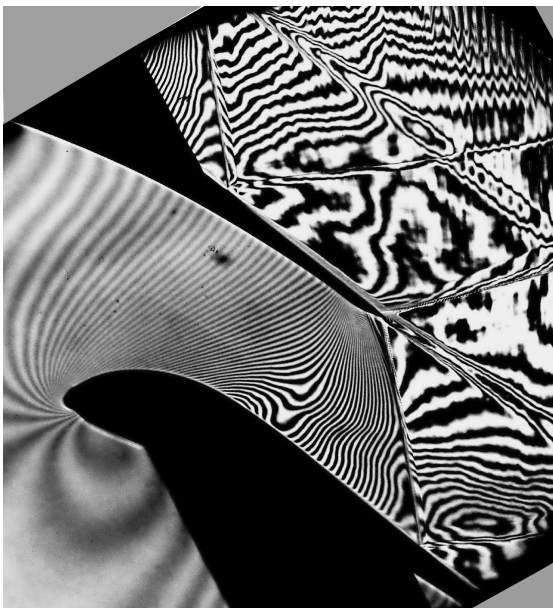


Figure 4: Interferogram showing shock wave/boundary layer interaction in the mid section of rotor turbine blade 48'' long at isentropic exit Mach number $M_{2is} = 1.348$, incidence angle $\tau = +30^\circ$.



Figure 5: Schlieren picture showing shock wave/boundary layer interaction in the mid section of rotor turbine blade 48'' long at isentropic exit Mach number $M_{2is} = 1.354$, incidence angle $\tau = -20^\circ$.

2 INTERACTION WITH THE BOUNDARY LAYER ON THE SUCTION SIDE

Interaction of a shock wave with the boundary layer on suction side of the blade occurs usually along the whole rotor blade in the last stage. The cambering of central lines of particular profiles of the blade changes along the blade height. This cambering depends on the changes of velocity triangles. Therefore, the surface of the suction side at hub or at the mid section is formed as convex and at the blade tip as concave.

The first example of shock wave/boundary layer interaction on the convex suction side of the profile is shown in Figures 4 and 5. Both photographs were taken under off-design condition of the flow in the tested cascade. The interferometric visualisation of the flow field in the mid section of the blade shows typical structure of interaction without flow separation when the boundary layer is most probably turbulent (see Fig. 4) [1]. Completely different situation regarding the structure of interaction is shown in the schlieren picture in Fig. 5. This interaction results in local flow separation and according to the length of the separated flow region, the boundary layer prior to interaction is probably laminar. During the interaction, the boundary layer changes to turbulent. These phenomena have impact on overall flow structure and the blade cascade losses. The difference between these two observed regimes lies in the great difference of the angle of incidence ($\Delta\iota = 50^\circ$). Detail of the recompression area downstream the sonic fringe in interferograms in Figures 6 and 7 show stronger compression near the boundary layer in case of the overloaded blade ($\iota = +30^\circ$, Fig. 6) in comparison with the situation in the Figure 7, where we can see situation in the flow field near the suction side at large negative incidence angle. The difference between these two situations in the recompression area is better apparent from the distribution of the Mach number on the suction side (Fig. 8) evaluated from the two interferograms (Figs. 6 and 7). This phenomenon together with both the different situation in the process of boundary layer forming at the leading edge area and the different length of stream line on the suction side upstream the interaction with shock wave might be the reasons for the position of transition and so for different behaviour of the boundary layer in the process of interaction with the internal branch of the exit shock wave.



Figure 6: Detail of the Figure 4: the recompression area on the suction side, mid section of rotor turbine blade 48'', isentropic exit Mach number $M_{2is} = 1.348$, incidence angle $\iota = +30^\circ$.

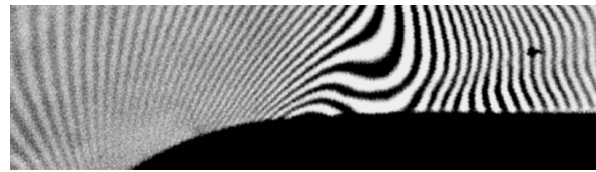


Figure 7: Interferogram related to schlieren picture in the Fig. 5: the recompression area on the suction side, mid section of rotor turbine blade 48'', isentropic exit Mach number $M_{2is} = 1.354$, incidence angle $\iota = -20^\circ$.

The numerical simulations of flow through the mid section of turbine blade 48'' were carried out by Rudas [2] or by Vachová [3]. In publication [3], the numerical simulations were carried out by the commercial code NUMECA using γRe transition model connected with the SST $k-\omega/k-\varepsilon$ turbulence model. Simulations of laminar and fully turbulent flow were also carried out for comparison. The calculated distribution of the skin friction coefficient along the profile chord with application of transition model is depicted in the diagram in Figure 9. The calculation shows the local boundary layer separation in the area of boundary layer interaction with shock wave, $x/c \sim (0.65 \div 0.7)$. Although CFD predicted local flow separation, extent of the separated flow

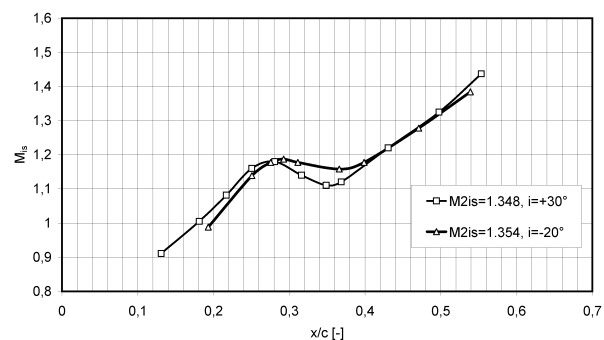


Figure 8: Isentropic Mach number distribution along the suction side near the recompression region at regimes shown in Figures 6 and 7.

region is under predicted (see Fig. 10 and [3]). Not even laminar calculation provided comparable extent of the separated flow region [3].

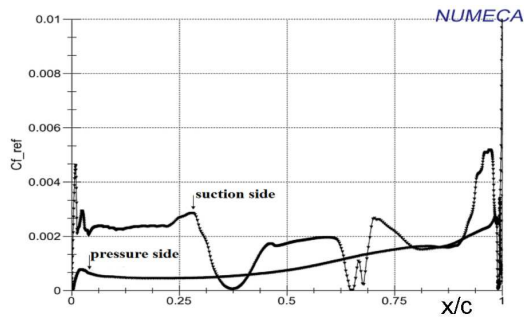


Figure 9: Distribution of skin friction coefficient along the blade profile - CFD simulation, transitional flow (Váchová [3])

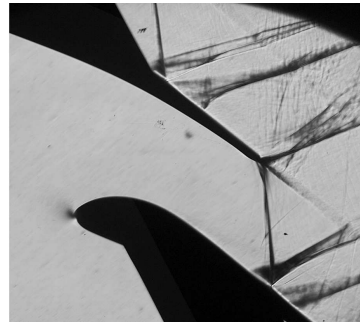


Figure 10: Schlieren picture, laminar boundary layer interaction with shock wave, incidence angle $i = 0^\circ$, $M_{2is} = 1.206$

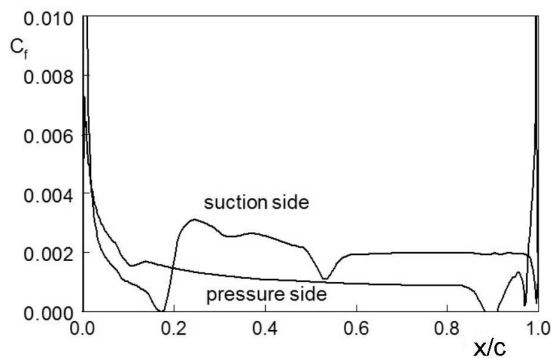


Figure 11: Distribution of friction coefficient C_f along the tip profile (long rotor blade 54"), $M_1 = 1.45$, $M_{2is} = 2.0$, CFD simulation (Straka, Příhoda [4]).

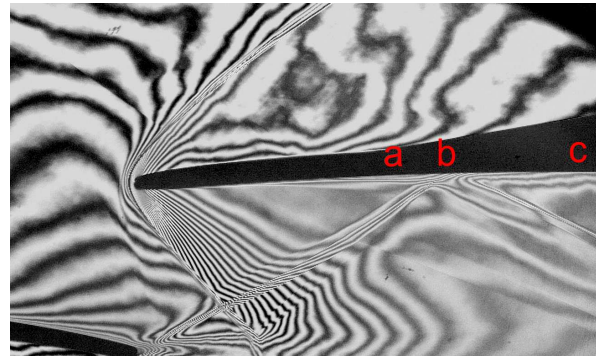


Figure 12: Interaction of internal branch of exit shock wave with boundary layer on suction side of neighbouring profile, (long rotor blade 60"), $M_1 = 1.886$, $M_{2is} = 2.096$.

Completely different situation occurs in case of the shock wave/boundary layer interaction on concave suction side in the tip section of the long turbine blade. The boundary layer is turbulent in the interaction area, nevertheless, the local separation bubble often occurs in the flow field near the point of interactions under off design conditions. Very strong expansion near the leading edge on suction side is followed by stagnation region in which the interaction takes place. Insufficient or negative gradient of static pressure along the suction side in the point just upstream of the interaction is typical for studied geometries of these tip profiles. According to the CFD simulations that were carried out by Straka and Příhoda [4], the boundary layer transition takes place commonly upstream the point of interaction (see Fig.11). The numerical simulation was carried out by means of the EARSM turbulence model according to Hellsten [5] completed by the bypass transition model with the algebraic equation for the intermittency coefficient proposed by Straka and Příhoda [6] and implemented into the in-house numerical code. The bypass transition on the suction side is

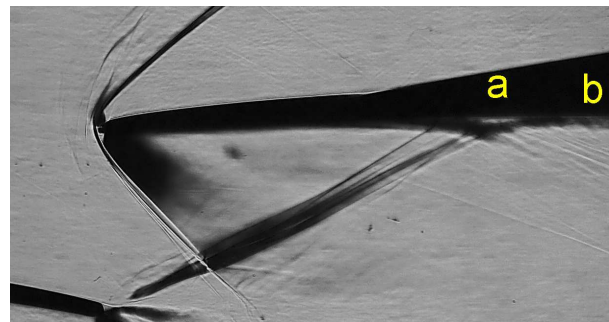
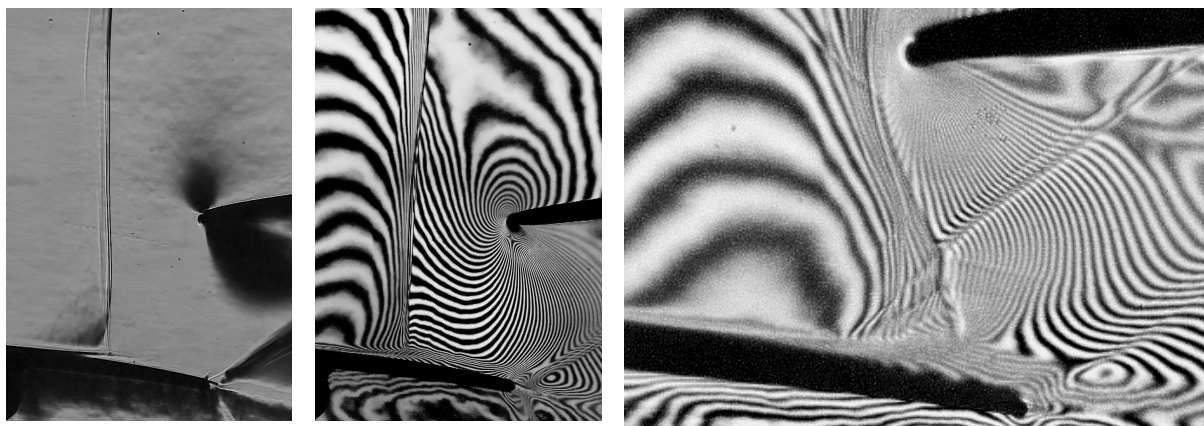


Figure 13: Interaction of internal branch of exit shock wave with boundary layer on suction side of neighbouring profile with separation bubble, (long rotor blade 60"), $M_1 = 2.012$, $M_{2is} = 2.149$.

evident from the distribution of C_f in the Fig. 11 ($x/c \sim 0.15$). The interaction of the boundary layer with inner branch of the exit shock wave can be seen in the C_f distribution at the distance $x/c \sim 0.5$ from the leading edge. The interferogram in the Figure 12 shows typical situation in the interaction area. In this region, thickness of the boundary layer (a) grows due to the adverse pressure gradient, the interaction with turbulent boundary layer (b) is more complex, and downstream the interaction, relatively very thick viscous shear layer (c) occurs. Transonic structures appearing in flow field in cascades representing tip sections of long turbine blades are generally extremely sensitive to changes of inlet and outlet parameters of flow. The schlieren picture in the Figure 13 shows situation in flow field at different inlet Mach number (or different incidence angle - unique incidence rule [7]) and different back pressure (in comparison with the flow parameters in Fig. 12). Local boundary layer separation (a) takes place in the area of interaction and very thick viscous shear layer develops downstream the interaction (b).



Schlieren picture

Interferogram

Figure 14: Interaction of internal branch of detached inlet normal shock wave with boundary layer on pressure side of neighbouring profile (tip section of long rotor blade 60"), $M_1 = 1.124$, $M_{2is} = 1.592$.

Figure 15: Complex interaction of internal branch of oblique inlet shock wave with boundary layer on pressure side of neighbouring profile (tip section of long rotor titanium blade 54"), $M_1 = 1.416$, $M_{2is} = 1.746$.

3 INTERACTION WITH THE BOUNDARY LAYER ON THE PRESSURE SIDE

This type of interaction appears commonly only in the tip region of ultra long turbine rotor blades (48", 54", 60"), where both the proper supersonic inlet velocity and suitable back pressure occurs. Interaction of internal branch of inlet shock wave with boundary layer on the pressure side in the tip section of rotor turbine blade 54" is described for example in [8]. It is typical for the pressure sides of investigated tip profiles, that the laminar/turbulent boundary layer transition takes place in the region of interaction with the inlet shock wave. An example of calculated distribution of friction coefficient along the pressure side is depicted in Fig. 11.

The interaction of detached normal inlet shock wave with boundary layer is shown in Fig. 14. These photographs were taken under off design condition at the cascade inlet and outlet. Both the schlieren picture and interferogram show local boundary layer separation and thick dissipative shear layer downstream the interaction. Increasing of the inlet Mach number leads to the attaching of inlet shock wave closely to leading edge and (by sufficiently low value of back pressure) to the bending of its inner branch. The point of interaction moves towards the trailing edge. The test results show that the interaction is more complex and local separation takes place once again (see Fig. 15). Impact of this complex interaction is that it suppresses the expansion area on the suction side of the neighbouring profile. Strong unsteady

behaviour of the flow field in the area of the interaction has been also observed. The sequence of interferograms, which were obtained by application of high speed CCD camera during interferometric measurement of tip cascade designed for blade 60" long, is shown in the Figure 16. Pictures were taken with frame frequency 6 kHz. The base of the shock wave moves cyclically upstream and downstream and the thickness of the shear layer downstream the interaction grows and decreases. This unsteady behaviour affects not only the cyclical changes of pressure distribution on pressure side but also the cyclical changes in the expansion in the region downstream the leading edge of the neighbouring profile (see the next chapter). As a result, cyclical torsion can occur in the region of the tip section of ultra long blade.

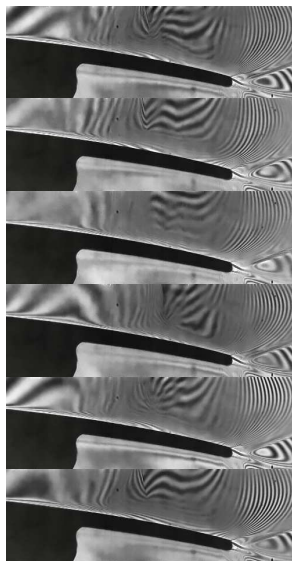


Figure 16: Unsteady interaction on pressure side (tip section of long rotor blade 60"), $M_1 = 1.124$, $M_{2is} = 1.797$, frame frequency 6 kHz.

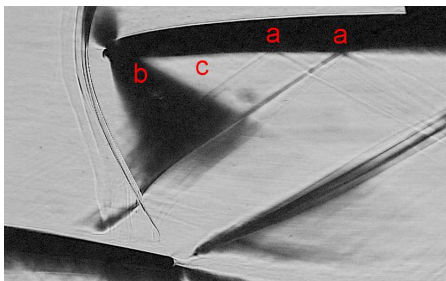


Figure 17: Complex interaction on the pressure and suction side (tip section of long rotor titanium blade 54"), schlieren picture, $M_1 = 1.45$, $M_{2is} = 2.0$.

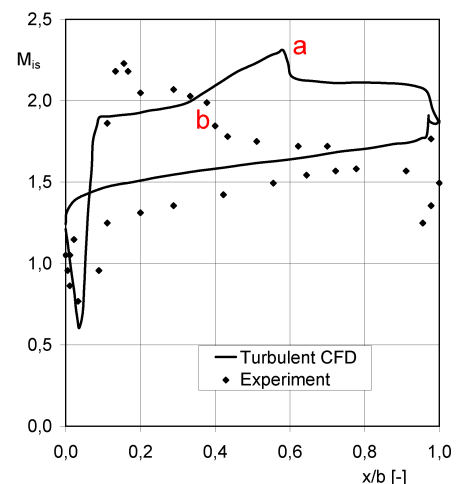


Figure 18: Distribution along the tip profile (tip section of long rotor titanium blade 54") obtained from experiment and by turbulent CFD simulation, $M_1 = 1.45$, $M_{2is} = 2.0$.

4 THE THIRD REGION OF THE INTERACTION

The possibility of the interaction of "reflected" shock wave (which arises from the interaction of the inner oblique part of inlet shock wave with the boundary layer on the pressure side) with boundary layer on the suction side (the third region of interaction – see Fig.3) is limited to the flow regimes in the tip region of long turbine blades with such an inlet Mach number and back pressure, which guarantees this interaction on the pressure side (or in the near wake area downstream the profile), and subsequently the formation of reflected wave.

Simple interaction without flow separation on the pressure side would guarantee expected additional supersonic expansion upstream the point (sign "a" in Fig. 17) where internal branch of exit shock wave interacts with boundary layer on the suction side. This solution (obtained by application of turbulent CFD procedure) is described by Rudas [2]. The additional supersonic expansion in experiment is suppressed, because the interaction of oblique part of inner branch of inlet shock wave with the laminar boundary layer on pressure side of neighbouring profile is much more complex [4] - see interferogram in Figure 15. Therefore, downstream the interaction of the inner branch of exit shock wave with boundary layer on suction side, the values of Mach number up to the trailing edge are significantly lower than in

the case of turbulent interaction on the pressure side (Fig. 18). This is also reason why the interaction of exit shock with the suction side boundary layer is located further upstream in experiment (sign "b" in Fig. 18). This fact has an essential negative influence on the aerodynamic loading of the studied profile. The interactions in the schlieren picture (sign "a" in the Figure 17) are interactions with turbulent boundary layer. Downstream the second interaction (and upstream the interaction with internal branch of exit shock wave) relatively thick dissipative layer develops. The region of the boundary layer transition is located next to the very strong supersonic expansion (sign "b" in Fig. 17) in the area (see "c" in Fig. 17) with practically neutral pressure gradient. This is in very good agreement with the result of numerical simulation (Straka, Příhoda [4]), where the transitional model was applied (see Fig. 11 in the paragraph 2). The distribution of the pressure coefficient C_p along the suction side of the profile obtained from experiment, turbulent CFD simulation (Fluent) and simulation, which was carried out by the in-house numerical code, are compared in the Fig. 19. Used in house code was based on the finite-volume solver for the RANS equations closed by the explicit algebraic model of Reynolds stresses completed by the modified algebraic transition model. The experimental data are evaluated from interferometric measurement, so the values of pressure coefficient are calculated from isentropic values of static pressure distribution on the profile. Although boundary conditions were not identical in these three cases, the differences between particular approaches show conclusively the complexity of the processes in the transonic flow field in investigated tip sections of ultra long turbine blades.

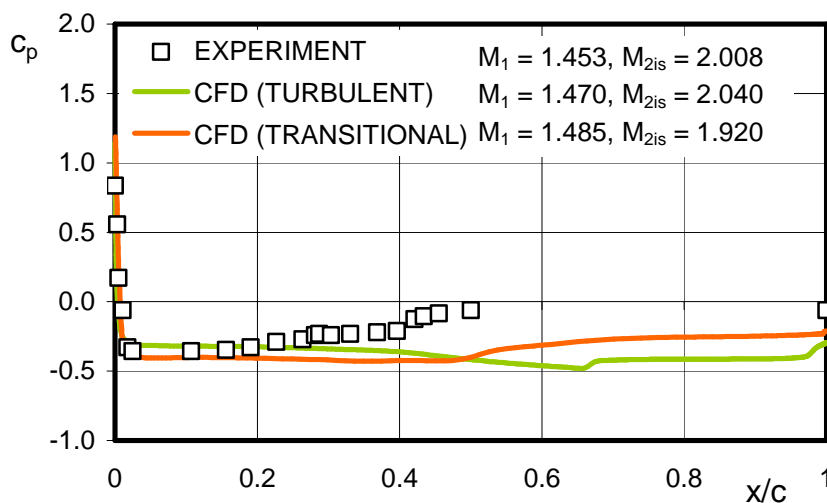


Figure 19: Distribution of the pressure coefficient along the suction side of tip profile obtained by in house code, commercial code and experiment, tip section of long rotor titanium blade 54".

5 CONCLUSIONS

The paper summarizes particular problems of boundary layer/shock wave interaction that is typical for modern ultra long rotor turbine blades and plays important role in case of recent designs of these blades.

Three basic situations have been shown, which appear in the inter blade channel: the interaction of internal branch of exit shock wave with boundary layer on suction side of the neighbouring profile; the interaction of internal branch of inlet shock wave with boundary layer on pressure side of the neighbouring profile; finally the interaction of "reflected" oblique

internal branch of inlet shock with boundary layer on suction side of the profile that generates the inlet shock wave.

Experimental data obtained from measurements on models of mid and tip section under design and off design conditions provide important information regarding complex and unsteady structures appearing in the transonic flow field within the boundary layer – shock wave interaction.

The application of different CFD procedures - commercial or developed “in house” proved that to predict the flow through such blade cascades correctly, it is necessary to employ transitional turbulence model when RANS is to be used. Results published in the paper show that the EARSM model performs reasonably well. The application of different experimental and numerical methods helps not only to validate numerical models and procedures but also to better understand physical phenomena, which appear in the measured flow fields as information provided by experiments is limited.

ACKNOWLEDGEMENTS

The work was supported by the Technology Agency of the Czech Republic under the grant TA03020277 and by the Czech Science Foundation under grant P101/12/1271. Institutional support RVO 61388998 is also gratefully acknowledged. The authors also thank DOOSAN ŠKODA POWER Co., Ltd., who made this research possible.

REFERENCES

- [1] Délerly J., Marvin J.G., (1986), Shock wave/boundary layer interactions, AGARDograph No. 280 Neuilly sur Seine, France, 222 p.
- [2] Luxa, M., Šimurda, D., Šafařík, P., Synáč, J., Rudas, B., (2013), High-speed aerodynamics investigation of the midsection of 48° Rotorblade for the last stage of steam turbine, In *10th European Conference on Turbomachinery - Fluid Dynamics and Thermodynamics*, Lappeenranta, pp360-369 : University of technology Lappeenranta, pp. 360-369.
- [3] Váchová, J., Luxa, M., Příhoda, J., Šimurda, D., (2015), Transition Model Application on Mid-Section Turbine Blade Cascade, In *Proceedings of the 12th International Symposium on Experimental Computational Aerothermodynamics of Internal Flows*, Lerici, pp. 1-8.
- [4] Luxa, M., Příhoda, J., Šimurda, D., Straka, P., Synáč, J., (2015) Investigation of the Compressible Flow through the Tip-Section Turbine Blade Cascade with Supersonic Inlet, In *Proceedings of the 12th International Symposium on Experimental Computational Aerothermodynamics of Internal Flows*. Lerici, pp. 1-8.
- [5] Hellsten, A., (2005), A new advanced k-omega turbulence model for high-lift aerodynamics, *AIAA Jour.*, 43, pp.1857-1869.
- [6] Straka, P., Příhoda, J., (2010), Application of the algebraic bypass-transition model for internal and external flows, *Proc. Conf. Experimental Fluid Mechanics 2010*, Liberec, pp.636-641.

- [7] Luxa, M., Rudas, B., Synáč, J., Šafařík, P., Šimurda, D., (2014), Experimental Technique for Setup of Supersonic Inlet Flow in a Profile Blade Cascade. In *The Application of Experimental and Numerical Methods in Fluid Mechanics and Energy 2014 - Proceedings of the International Conference*, Žilina, pp.149-152.
- [8] Luxa, M., Šimurda, D., Fořt, J., Fürst, J., Šafařík, P., Synáč, J., Rudas, B., (2015), Aerodynamic Investigation of Tip Section for Titanium Blade 54", Proceedings of the 11th European Conference on Turbomachinery Fluid Dynamics and Thermodynamics (ETC11), Madrid.